Inorganic Chemistry

Article

pubs.acs.org/IC

Crystal Structure Analysis of $La_2Ni_6CoD_x$ During Deuterium Absorption Process

Kenji Iwase,*[,†] Kazuhiro Mori,[‡] Suguru Tashiro,[†] Hitoshi Yokota,[†] and Tetsuya Suzuki[†]

[†]Department of Materials Science and Engineering, Ibaraki University, 4-12-1, Nakanarusawa, Hitachi 316-8511, Japan

[‡]Research Reactor Institute, Kyoto University, 2-1010 Asashiro-nishi, Kumatori, Sennan, Osaka 590-0494, Japan

ABSTRACT: The crystal structures of $La_2Ni_6CoD_x$ (x = 5.2 and 9.6) were determined by *in situ* neutron diffraction along the P−C isotherm. $La_2Ni_6CoD_{5.2}$ (phase I) was found to be orthorhombic with lattice parameters a = 0.500670(2) nm, b = 0.867211(4) nm, and c = 2.99569(7) nm. The 10 deuterium sites were located in the $MgZn_2$-type and $CaCu_5$-type cells, with deuterium contents of 0.95 D/M and 0.39 D/M, respectively. The full deuteride $La_2Ni_6CoD_{9.6}$ (phase II) was monoclinic with lattice parameters a = 0.516407(3) nm, b = 0.894496(6) nm, c = 3.11206(1) nm, and β = 90.15(1)°. The phase II had 11 sites for deuterium occupation. The deuterium contents of the $MgZn_2$-type and the $CaCu_5$-type cell were 1.63 D/M and 0.78 D/M, respectively. The sequence of phase transformation of La_2Ni_6Co was hexagonal, followed by orthorhombic (phase I), and then monoclinic (phase II), for the first absorption process. The phase transformation resulted in lowered symmetry and the variation of deuterium atom occupation.

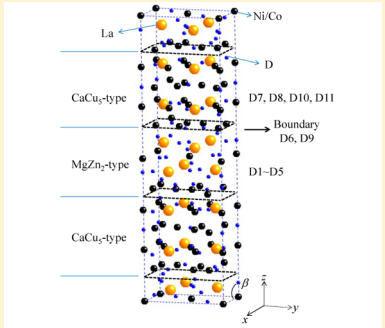

Crystal structure of $La_2Ni_6CoD_{9.6}$

1. INTRODUCTION

La−Ni intermetallic compounds have been investigated as hydrogen storage materials. The phase diagram of the La−Ni system shows nine phases in the equilibrium state: La_3Ni, La_7Ni_3, LaNi, La_2Ni_3, La_7Ni_{16}, $LaNi_3$, La_2Ni_7, La_5Ni_{19}, and $LaNi_5$.[1,2] Among them, superlattice alloys $LaNi_3$, La_2Ni_7, and La_5Ni_{19} consist of cells with $MgZn_2$-type and $CaCu_5$-type structures stacked along the c-axis in ratios of 1:1 to 1:3. $LaNi_3$ shows a rhombohedral $PuNi_3$-type structure with lattice parameters of a = 0.5083 nm and c = 2.509 nm.[3] La_2Ni_7 has two types of crystal structure: a hexagonal Ce_2Ni_7-type structure with a = 0.5058 nm and c = 2.471 nm, or a rhombohedral Gd_2Co_7-type structure with a = 0.5056 nm and c = 3.698 nm.[3,4] La_5Ni_{19} shows a rhombohedral Ce_5Co_{19}-type structure.[2]

We previously reported the hydrogenation property of Ce_2Ni_7-type La_2Ni_7 by means of *in situ* X-ray diffraction (XRD).[5] In the first absorption process, the plateau was observed at 0.57 MPa. The maximum hydrogen capacity reached 1.24 H/M, but after the first desorption process 0.74 H/M of hydrogen remained in the sample. The reversible capacity is small. The metal sublattice of La_2Ni_7 changes with increasing hydrogen content to orthorhombic ($Pbcn$) at $La_2Ni_7H_{7.1}$ and monoclinic ($C2/c$) at $La_2Ni_7H_{10.8}$.

Colinet and Pasturel reported the P−C isotherm of $LaNi_{5-x}Co_x$ at 298 K.[6] $LaNi_3Co_2$ showed two plateaus in the absorption−desorption isotherm. The first plateau appeared at 0.02 MPa and the second at 0.6 MPa in the P−C isotherm of 298 K. The length of the first plateau is 6 times wider than the second plateau. The enthalpy of the hydrogenation reaction was −40 kJ/mol H_2, compared with −32 kJ/mol H_2 for $LaNi_5$. It is also noted that the pressure in the first plateau decreased with increasing Co substitution.

Nakamura et al. reported the phase transformation in $LaNi_3Co_2$ with the $CaCu_5$-type structure ($P6/mmm$), upon hydrogenation, by *in situ* XRD.[7] The alloy showed α (hexagonal: $P6/mmm$), β (orthorhombic: $Cmmm$), γ (orthorhombic: $Im2m$), and δ (hexagonal: $P6/mmm$) hydride phases with increasing hydrogen content. The phase transformation was accompanied by anisotropic lattice expansion. $LaNi_5$ with the hexagonal $P6/mmm$ structure transformed to $LaNi_5D_7$ with $P6_3mc$ space group,[8,9] while the phase transformation of $LaNi_3Co_2$ with increasing hydrogen content was different from $LaNi_5$.

This paper presents results of *in situ* neutron diffraction measurement of $La_2Ni_6CoD_x$ (x = 5.2 and 9.6) during first absorption. It is of interest whether the phase transformation and deuterium atom occupation of La_2Ni_7-based superlattice alloy are affected by substitution of Co for Ni. In order to clarify the phase transformation along the P−C isotherm, deuterium atom positions and occupancies were refined by the Rietveld method. The volumes of the unit cell, and the $MgZn_2$-type and $CaCu_5$-type cells, expand anisotropically depending on the deuterium location and occupation. Deuterium atoms occupy interstitial sites in the metal lattice, and the related polyhedrons are deformed by deviation of deuterium atoms from the centers of these polyhedrons. The deuterium distribution of the $MgZn_2$-type and $CaCu_5$-type cells is related to the phase transformation. It is necessary to refine the structural parameters during the deuterium absorption process.

Received: June 8, 2015
Published: August 12, 2015

DOI: 10.1021/acs.inorgchem.5b01290
Inorg. Chem. 2015, 54, 8650−8655

2. EXPERIMENTAL SECTION

La_2Ni_6Co alloy was prepared by arc-melting La, Ni, and Co metals (99.9%) in an Ar atmosphere. The obtained ingot was annealed at 1153 K for 63 h under reduced pressure (2.0×10^{-2} Pa) and quenched in ice water. The P−C isotherm was measured using the Sieverts method. The sample was evacuated at 393 K for 1 h before deuteride for pretreatment of activation.

Neutron diffraction data were taken on a TOF (time-of-flight) diffractometer iMATERIA[10−12] at J-PARC in Japan. The diffractometer views a liquid hydrogen moderator and has an incident flight path of 26.5 m. The high-resolution diffraction pattern was recorded by a backward detector bank located 1.9 m from the sample position. The detector bank contains 416 one-dimensional ^{3}He PSDs (position sensitive detectors). The obtained diffraction pattern covers the d range 0.018−0.5 nm with resolution of $\Delta d/d$ = 0.16%. The Rietveld refinement program for TOF neutron diffraction, Z-Rietveld, was used to analyze the diffraction data.[13,14]

In situ neutron diffraction data were taken using a vanadium sample holder with a 2 μm copper coating on the inner surface to prevent reaction with hydrogen.[15] The vanadium can was 70 mm long, with 8 mm inner diameter and 0.3 mm wall thickness. A 4.2 g sample was loaded in the sample holder.

3. RESULTS

3.1. Crystal Structure of La_2Ni_6Co. The structural parameters of the alloy were determined by Rietveld refinement of the neutron diffraction data in the d region between 0.05 and 0.45 nm. The diffraction pattern of La_2Ni_6Co is shown in Figure 1, along with those of the deuteride phases I and II. The

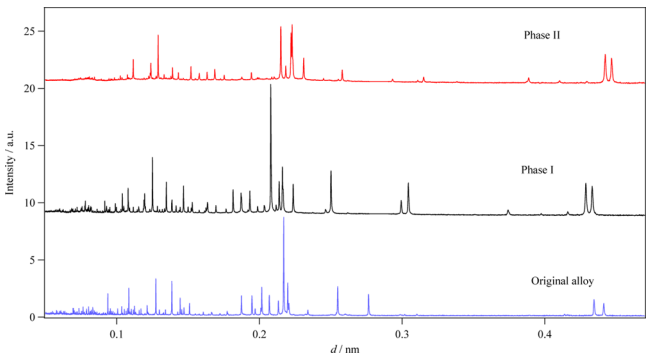

Figure 1. Neutron diffraction patterns of the original alloy, La_2Ni_6Co, and deuteride phases I and II.

model was based on the Ce_2Ni_7-type structure with space group $P6_3/mmc$ (No. 194) reported for La_2Ni_7.[4,5] Co atoms substitute only Ni at 6*h* site of the $z = {}^1/_4$ plane inside the $CaCu_5$-type cell, which provided a not good agreement with the observed pattern. The same tendency was also seen in other Ni sites of both $MgZn_2$-type cell and $CaCu_5$-type cell. Then the substituted Co atoms were assumed to be located randomly at the Ni site of 2*a*, 4*e*, 4*f*, 6*h*, and 12*k*, with a ratio of 0.14:0.86; this one agreed fairly well with the observed data. The refined lattice parameters were a = 0.507 121(5) nm and c = 2.470 58(5) nm.

3.2. P−C Isotherm of La_2Ni_6Co-D System. The P−C isotherm of La_2Ni_6Co for the first absorption−desorption process at 298 K is shown in Figure 2. In the absorption process, the equilibrium pressure increased gradually up to 0.7 D/M and showed a plateau between 0.7 and 1.0 D/M. The plateau pressure was approximately 0.4 MPa. The maximum deuterium capacity reached 1.1 D/M at 1.0 MPa. The P−C isotherm of desorption and absorption differed. The plateau

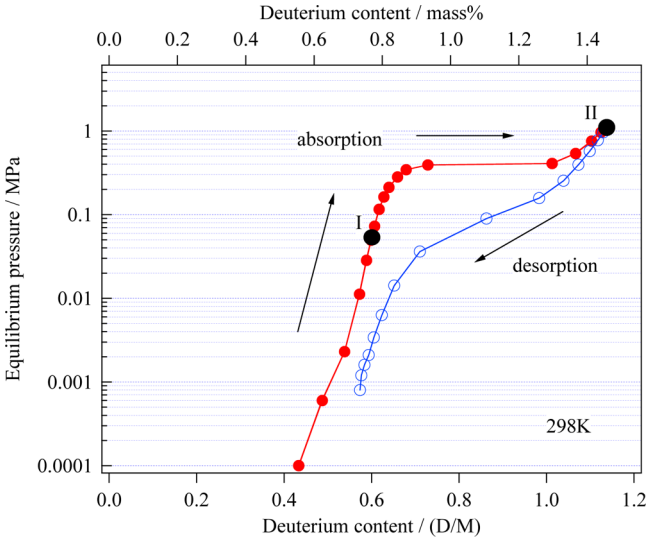

Figure 2. Pressure−composition isotherms of the La_2Ni_6Co-D system for the first absorption−desorption process at 298 K.

region was not observed in the desorption process. After the desorption measurement, 0.57 D/M of deuterium remained in the alloy. The hydrogenation property of La_2Ni_6Co was similar to that of La_2Ni_7.[5]

3.3. Diffraction Profile Change During Deuterium Absorption Process. *In situ* neutron diffraction patterns of the original alloy and two deuteride phases (phase I and phase II indicated in the P−C isotherm of Figure 2) are shown in Figure 1. The deuterium contents were approximately 0.6 D/M and 1.1 D/M. The three diffraction profiles are clearly different from each other, indicating structural transformation as deuterium content increased.

3.4. Structural Analyses of Phase I and Phase II. Yartys et al. reported the crystal structure of $La_2Ni_7D_{6.5}$ by *ex situ* neutron diffraction.[16] They reported that $La_2Ni_7D_{6.5}$ had the same hexagonal symmetry ($P6_3/mmc$) as the original alloy. In this work, an initial structural model of $La_2Ni_6CoD_{5.2}$ (phase I), based on the same model as $La_2Ni_7D_{6.5}$, was developed. The calculated pattern did not fit well with the observed pattern; the goodness of fit parameter S was 9.5.

The structural model of the metal sublattice of $La_2Ni_7H_{7.1}$ with an orthorhombic *Pbcn* (No. 60) symmetry has been reported by XRD.[5] The diffraction data of $La_2Ni_6CoD_{5.2}$ (phase I) was analyzed with this model, allocating appropriate deuterium occupancies. The model gave a good fit as shown in Figure 3. The refined structural parameters and the R factors are listed in Table 1. The refined lattice parameters were a = 0.500670(2) nm, b = 0.867211(4) nm, and c = 2.99569(7) nm. The $La_2Ni_6CoD_{5.2}$ crystal structure is shown in Figure 4. Deuterium atoms occupy both $MgZn_2$-type and $CaCu_5$-type cells. We have determined 10 sites for deuterium occupation in $La_2Ni_6CoD_{5.2}$ by Rietveld refinement. D1, D2, and D4−D6 atoms occupy the $MgZn_2$-type cell as shown in Figure 4. D2 and D4 occupy the $La_3(Ni/Co)$ tetrahedral site. The occupation factors of those tetrahedral sites were approximately 0.49. D1 and D6 atoms occupy the $La_3(Ni/Co)_3$ octahedral site, and D5 atoms occupy the $La_3(Ni/Co)_2$ pentahedral site. D7, D8, and D10 atoms are located in the $CaCu_5$-type cell. D7 atoms occupy the 4*c* site of the $La_2(Ni/Co)_2$ tetrahedral site. D8 atoms are located at the $La_2(Ni/Co)_4$ octahedral site with an occupation factor of g = 0.95(4), the maximum value in the

DOI: 10.1021/acs.inorgchem.5b01290
Inorg. Chem. 2015, 54, 8650−8655

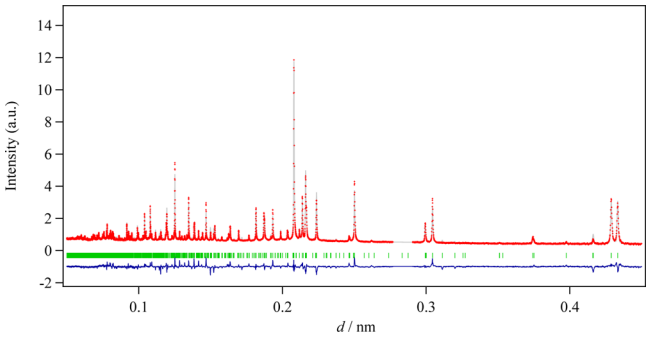

Figure 3. Rietveld refinement of neutron diffraction data for orthorhombic $La_2Ni_6CoD_{5.2}$. The solid line indicates the calculated intensities, with superimposed points denoting the observed intensities. Data *d* values around 0.28 nm, which contained irrational peaks from frame overlaps of neutrons, were excluded from the refinement.

deuterium occupation of the $La_2Ni_6CoD_{5.2}$. D10 atoms occupy the $La_2(Ni/Co)_3$ pentahedral site. D3 and D9 are located at the $La_2(Ni/Co)_2$ site near the boundary between the $MgZn_2$-type and the $CaCu_5$-type cells. The deuterium content of the $MgZn_2$-type cell indicated 0.95 D/M, more than double that of the $CaCu_5$-type cell (D/M = 0.39).

The monoclinic model with space group *C*2/*c* (No. 15) was adopted for $La_2Ni_6CoD_{9.6}$ (phase II). This model was reported for the metal sublattice of $La_2Ni_7H_{10.8}$ by XRD.[5] The Rietveld refinement pattern of $La_2Ni_6CoD_{9.6}$ is shown in Figure 5, with the structural parameters shown in Table 2. The refined lattice parameters were a = 0.516 40 (3) nm, b = 0.894 496(6) nm, c = 3.112 06 (1) nm, and β = 90.15(1)°. As shown in Figure 6, D1−D5 atoms were located in the $MgZn_2$-type cell, and D7, D8, D10, and D11 atoms in the $CaCu_5$-type cell. Deuterium atoms occupied the 8*f* and 4*e* sites as shown in Table 2. The occupation factors of D1−D3, D8, D10, and D11 were 0.90(2)−0.98(1), indicating almost full occupation. The other five deuterium atoms had lower occupations around 0.8−0.9.

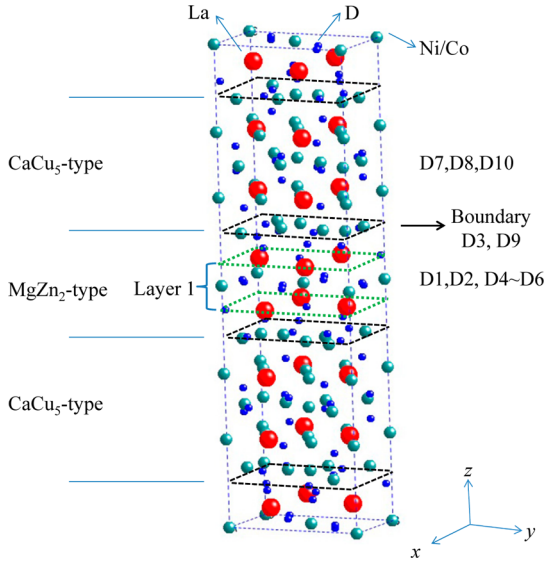

Figure 4. Crystal structure of $La_2Ni_6CoD_{5.2}$ with *Pbcn* symmetry.

D6 and D9 atoms located in the boundary between the $MgZn_2$-type and $CaCu_5$-type cells had occupation factors g(D6) = 0.85(4) and g(D9) = 0.91(3). The analysis indicated that the deuterium contents of the $MgZn_2$-type and $CaCu_5$-type cells were 1.63 D/M and 0.78 D/M, respectively.

4. DISCUSSION

4.1. $La_2Ni_6CoD_{5.2}$ with Orthorhombic Structure. Yartys et al. reported the crystal structure of $La_2Ni_7D_{6.5}$ using neutron diffraction,[16] where the structural model was based on space group $P6_3/mmc$ of the original alloy. The volume expansions of the $MgZn_2$-type cell, the $CaCu_5$-type cell, and the unit cell from the original alloy were −3.0%, 47.8%, and 14.9%, respectively. The deuterium content of the $MgZn_2$-type cell was approximately 1.6 D/M, while the absorbed deuterium atom

Table 1. Structural Parameters of $La_2Ni_6CoD_{5.2}$[a]

atom	site	g	x	y	z	B (10^{-2} nm^2)
La1	8*d*	1	0.000(1)	0.331(2)	0.186(1)	0.7(1)
La2	8*d*	1	0.000(2)	0.335(4)	0.046(7)	3.7(3)
(Ni/Co)1	4*a*	0.86/0.14	0	0	0	2.0(7)
(Ni/Co)2	8*d*	0.86/0.14	0.500(1)	0.164(3)	0.183(5)	0.4(2)
(Ni/Co)3	4*c*	0.86/0.14	0	0.835(8)	$^1/_4$	0.6(4)
(Ni/Co)4	8*d*	0.86/0.14	0.242(3)	0.082(7)	0.250(1)	0.2(5)
(Ni/Co)5	8*d*	0.86/0.14	0.000	0.832(7)	0.110(2)	0.2(3)
(Ni/Co)6	8*d*	0.86/0.14	0.251(6)	0.078(3)	0.114(3)	0.2(2)
(Ni/Co)7	8*d*	0.86/0.14	0.746(1)	0.085(3)	0.118(9)	0.1(3)
(Ni/Co)8	8*d*	0.86/0.14	0.000(1)	0.000(1)	0.181(7)	0.7(5)
D1	8*d*	0.45(4)	0.444(5)	0.475(8)	0.077(2)	3.7(7)
D2	8*d*	0.48(2)	0.501(1)	0.333(1)	0.015(3)	1.5(5)
D3	8*d*	0.49(1)	0.478(1)	0.683(5)	0.103(1)	2.2(4)
D4	8*d*	0.49(1)	0.270(2)	0.394(1)	0.990(2)	1.5(5)
D5	8*d*	0.48(2)	0.494(6)	0.521(9)	0.050(2)	1.0(3)
D6	8*d*	0.45(3)	0.957(3)	0.675(5)	0.080(6)	0.8(2)
D7	4*c*	0.85(4)	0	0.183(2)	$^1/_4$	4.4(8)
D8	8*d*	0.95(4)	0.569(4)	0.324(1)	0.161(7)	3.5(4)
D9	8*d*	0.48(1)	0.530(1)	0.770(3)	0.118(7)	1.2(2)
D10	8*d*	0.47(2)	0.500(3)	0.000(1)	0.275(1)	4.0(3)

[a]Space group: *Pbcn* (No. 60), a = 0.500 670(2) nm, b = 0.867 211(4) nm, and c = 2.995 69(7) nm. R_{wp} = 7.6%, R_p = 4.8%, R_e = 1.4%, and S = 5.5.

DOI: 10.1021/acs.inorgchem.5b01290
Inorg. Chem. 2015, 54, 8650−8655

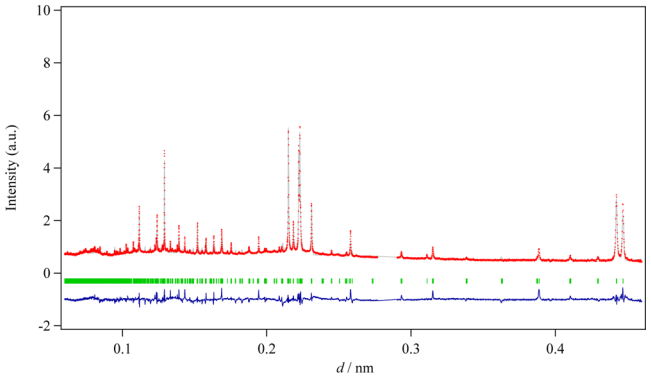

Figure 5. Rietveld refinement of neutron diffraction data for monoclinic $La_2Ni_6CoD_{9.6}$. Data d values around 0.28 nm were excluded from the refinement.

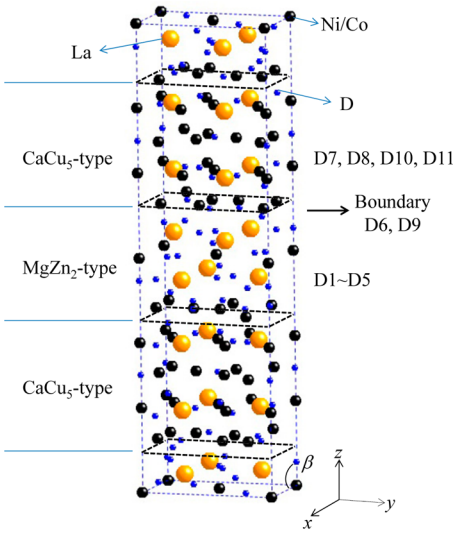

Figure 6. Crystal structure of $La_2Ni_6CoD_{9.6}$ with $C2/c$ symmetry.

did not exist in the $CaCu_5$-type cell. Deuterium atoms occupy the La_3Ni_3 octahedral sites and the La_3Ni_1 and La_2Ni_2 tetrahedral sites of the $MgZn_2$-type cell.

The expansion of lattice axes, the unit cell of $La_2Ni_6CoD_{5.2}$, and the volumes of $MgZn_2$-type and $CaCu_5$-type cells are listed in Table 3. The lattice expanded anisotropically during transformation from the alloy to phase I; the elongation of the c axis was marked. The volume expansions of the $MgZn_2$-type cell, the $CaCu_5$-type cell, and the unit cell from the alloy were 49.8%, 1.9%, and 18.2%, respectively. The result is similar to that of La_2Ni_7.[5] The deuterium contents of the $MgZn_2$-type cell and the $CaCu_5$-type cell were 0.95 D/M and 0.39 D/M, respectively, a result comparable with that of $La_2Ni_7D_{6.5}$.[16] Deuterium atoms occupy only the $MgZn_2$-type cell of $La_2Ni_7D_{6.5}$.[16] The occupation factors of D3 and other D atoms are 0.5 and 1. Considering the deuterium atomic position and the occupation factor, Westlake's criterion for H−H distance (0.21 nm) is not satisfied.[17] The two results indicate a wide discrepancy. In our results, the volume expansion and the deuterium content of the $MgZn_2$-type cell are evidently larger than those of the $CaCu_5$-type cell. Now we focus on the deuterium occupation of D2, D4, and D5. D2 and D4 atoms occupy the La_3Ni_1 tetrahedral site, and D5 atoms occupy the La_3Ni_2 pentahedral site. These polyhedrons are deformed in comparison with the original alloy. The D2−D4, D2−D5, and D4−D5 distances are 0.148, 0.193, and 0.183 nm, which do not satisfy Westlake's criterion.[17] The occupation factors of D2, D4, and D5 are under 0.5. If the D2 atom occupies the 8d site, the nearest neighbor 8d sites for D4 and D5 atoms cannot be occupied. D2 and D4 atoms are located in layer 1 in the $MgZn_2$-type cell as shown in Figure 4. Layer 1 exhibits anisotropic expansion along the c-axis with volume expansion of

Table 2. Structural Parameters of $La_2Ni_6CoD_{9.6}$[a]

atom	site	g	x	y	z	B (10^{-2} nm^2)
La1	8f	1	0.000(1)	0.321(7)	0.321(1)	1.7(1)
La2	8f	1	0.000(2)	0.330(2)	0.456(3)	3.2(3)
(Ni/Co)1	4a	0.86/0.14	0	0	0	2.1(2)
(Ni/Co)2	8f	0.86/0.14	0.000(2)	0.000(1)	0.180(2)	0.3(2)
(Ni/Co)3	8f	0.86/0.14	0.000(3)	0.656(5)	0.180(2)	1.2(2)
(Ni/Co)4	8f	0.86/0.14	0.256(6)	0.595(2)	0.250(1)	0.6(2)
(Ni/Co)5	4e	0.86/0.14	0	0.834(1)	$^1/_4$	2.7(2)
(Ni/Co)6	8f	0.86/0.14	0.500(2)	0.322(4)	0.117(2)	0.8(2)
(Ni/Co)7	8f	0.86/0.14	0.263(7)	0.573(7)	0.109(2)	0.2(1)
(Ni/Co)8	8f	0.86/0.14	0.755(4)	0.576(2)	0.110(4)	0.2(1)
D1	8f	0.90(2)	0.496(5)	0.500(1)	0.450(6)	2.5(2)
D2	8f	0.94(1)	0.750(2)	0.750(2)	0.000(1)	3.5(7)
D3	8f	0.94(3)	0.761(5)	0.578(1)	0.052(1)	2.3(2)
D4	8f	0.80(5)	0.252(5)	0.572(7)	0.016(4)	1.1(2)
D5	8f	0.82(5)	0.000(4)	0.640(7)	0.416(3)	3.0(4)
D6	8f	0.85(4)	0.778(1)	0.370(2)	0.388(7)	1.3(4)
D7	4e	0.88(4)	0	0.000(3)	$^1/_4$	2.3(2)
D8	8f	0.94(2)	0.525(5)	0.325(6)	0.170(4)	2.1(3)
D9	8f	0.91(3)	0.275(7)	0.760(1)	0.108(6)	2.3(2)
D10	8f	0.98(1)	0.278(3)	0.565(2)	0.157(5)	3.6(6)
D11	8f	0.96(3)	0.764(1)	0.566(5)	0.191(6)	1.2(5)

[a]Space group: $C2/c$ (No. 15), a = 0.516 407(3) nm, b = 0.894 496(6) nm, c = 3.112 06(1) nm, and β = 90.15(1)°. R_{wp} = 6.3%, R_p = 4.6%, R_e = 1.2%, and S = 5.3.

DOI: 10.1021/acs.inorgchem.5b01290
Inorg. Chem. 2015, 54, 8650−8655

Table 3. Expansion of Lattice Axes, Unit Cell Volumes, and Volumes of the $MgZn_2$-Type and $CaCu_5$-Type Cells[a]

	expansion 1 (%) alloy → I	expansion 2 (%) I → II	expansion 3 (%) alloy → II
a	−1.3	3.2	1.8
b	−1.3	3.2	1.8
c	21.3	4.2	26.0
unit cell volume	18.2	10.8	30.6
$CaCu_5$-type cell	1.9	11.3	13.4
$MgZn_2$-type cell	49.8	8.4	62.4

[a]Expansions 1, 2, and 3 refer to those from original alloy to phase I, phase I to phase II, and original alloy to phase II, respectively.

81%. It is suggested that La_2Ni_6Co with a hexagonal structure ($P6_3/mmc$) transforms into $La_2Ni_6CoD_{5.2}$ with orthorhombic structure (*Pbcn*) by the anisotropic volume expansion of the $MgZn_2$-type cell. D2 and D4 atoms occupy the La_3Ni_1 tetrahedral site, because La exhibits a high affinity for H.

4.2. $La_2Ni_6CoD_{9.6}$ with Monoclinic Structure. The expansions of the lattice axes and the unit cell of $La_2Ni_6CoD_{9.6}$ are listed in Table 3. The lattice expands almost isotropically during transformation from phase I to phase II, with the *a*, *b*, and *c* axes expanding by 3.2−4.2%. The volume expansions of $MgZn_2$-type cell, $CaCu_5$-type cell, and the unit cell are 8.4%, 11.3%, and 10.8%, respectively. The deuterium positions and the occupation factors were determined (Table 2). The deuterium occupation factors of all sites exceeded 0.80. The deuterium content of the $MgZn_2$-type and $CaCu_5$-type cells was 1.63 D/M and 0.78 D/M, respectively. The deuterium contents of both cells increased during phase transformation from phase I to the phase II. D7 atoms occupied the 4*e* site of the Ni_5 pentahedron in $CaCu_5$-type cell. The pentahedral site consists only of Ni. The occupation sites of phase I were formed by La and Ni atoms. The deuterium occupation sites in the $CaCu_5$-type cell are pentahedral (Ni_5, La_2Ni_3) and octahedral (La_2Ni_4). These sites are deformed evidently in comparison with the original alloy and the phase I. The same tendency is also seen in the $MgZn_2$-type cell.

4.3. Deuterium Content of $MgZn_2$-Type Cell and $CaCu_5$-Type Cell. Guzuki et al. reported the crystal structure and the P−C isotherm of $La_{1.63}Mg_{0.37}Ni_7$ with Ce_2Ni_7-type structure.[18] Deuterium atom positions and occupancies of $La_{1.63}Mg_{0.37}Ni_7D_{8.8}$ were refined by *ex situ* neutron diffraction. $La_{1.63}Mg_{0.37}Ni_7D_{8.8}$ had the same hexagonal symmetry ($P6_3/mmc$) as the original alloy. The deuterium contents of the $MgZn_2$-type and the $CaCu_5$-type cell were 1.31 D/M and 0.86 D/M, respectively. The maximum deuterium capacity reached 0.97 D/M. Zhang et al. reported the crystal structure of $Ca_3Mg_2Ni_{13}$ deuteride and the P−C isotherm.[19] The maximum deuterium capacity reached 0.87 D/M. $Ca_3Mg_2Ni_{13}D_{15.6}$ was taken by *in situ* neutron diffraction at deuterium pressure 2.9720 MPa. The structure of the deuteride phase was the same symmetry ($R\bar{3}m$) as the original alloy. The deuterium contents of the $MgZn_2$-type and the $CaCu_5$-type cell were 0.9 D/M and 0.8 D/M. The crystal structure of Nd_2MgNi_9 deuteride and the P−C isotherm were reported by Yartys and Denys.[20] $Nd_2MgNi_9D_{11.9}$ was taken by *in situ* neutron diffraction. The refined structural model was $PuNi_3$-type, which was the same symmetry as the original alloy. The deuterium content of the $MgZn_2$-type and the $CaCu_5$-type cell were 0.93 D/M and 1.05 D/M. In this study, the full deuteride $La_2Ni_6CoD_{9.6}$ was monoclinic ($C2/c$), which was the different symmetry ($P6_3/mmc$) as the original alloy. The deuterium content of the $MgZn_2$-type cell indicated 1.63 D/M, more than double that of the $CaCu_5$-type cell (D/M = 0.78).

Mg atoms substitute La, Ca, and Nd sites of $MgZn_2$-type cell. The difference of the deuterium content between the $MgZn_2$-type cell and the $CaCu_5$-type cell decreases by Mg substitution. The plateau region of Mg-substitution alloy was larger than that of Mg-free alloy.[21] The phase transition is not observed in Mg-substitution alloy, which may be related to the deuterium content of the $MgZn_2$-type cell and the $CaCu_5$-type cell.

5. CONCLUSIONS

We investigated the crystal structure and the phase transformation of $La_2Ni_6CoD_x$ (x = 5.2 and 9.6) during the first absorption process by *in situ* neutron diffraction. The phase I of $La_2Ni_6CoD_{5.2}$ has an orthorhombic *Pbcn* structure (a = 0.500670(2) nm, b = 0.867211(4) nm, and c = 2.99569(7) nm) with 10 deuterium sites: five sites exist in the $MgZn_2$-type cell, three in the $CaCu_5$-type cell, and two in the boundary between the cells. The deuterium contents of the $MgZn_2$-type cell and $CaCu_5$-type cell were 0.95 D/M and 0.39 D/M, respectively. The phase II of $La_2Ni_6CoD_{9.6}$ is described by a monoclinic structure with space group $C2/c$. The lattice parameters are a = 0.516 407 (3) nm, b = 0.894 496(6) nm, c = 3.112 06 (1) nm, and β = 90.15 (1)°. The deuterium atoms occupy 11 sites: five sites in the $MgZn_2$-type cell, four in the $CaCu_5$-type cell, and two sites in the boundary between the cells. The deuterium contents of the $MgZn_2$-type cell and $CaCu_5$-type cell were 1.63 D/M and 0.78 D/M, respectively. The deuterium content of the $MgZn_2$-type cell in phase I and phase II is clearly larger than that of the $CaCu_5$-type cell. The phase transformation of La_2Ni_6Co followed the order hexagonal, orthorhombic (phase I), and then monoclinic (phase II), for the first absorption process, accompanied by anisotropic lattice expansion.

AUTHOR INFORMATION

Corresponding Author

*E-mail: fbiwase@mx.ibaraki.ac.jp. Phone: +81-294-38-5327. Fax: +81-294-38-5226.

Notes

The authors declare no competing financial interest.

ACKNOWLEDGMENTS

The authors wish to thank Emeritus Professor H. Asano (University of Tsukuba) for the helpful advice, and Dr. T. Ishigaki (Ibaraki University) and Dr. A. Hoshikawa (Ibaraki University) for technical assistance in neutron diffraction. This work was supported by a Grant-in-Aid for Creative Scientific Research (No. 25790080) from the Ministry of Education, Culture, Sports, Science, and Technology of Japan.

DOI: 10.1021/acs.inorgchem.5b01290
Inorg. Chem. 2015, 54, 8650−8655

REFERENCES

(1) *Binary Alloy Phase Diagrams*, 2nd ed., plus updates; Okamoto, H., Ed.; ASM International: Materials Park, OH, 1990.
(2) Yamamoto, T.; Inui, H.; Yamaguchi, M.; Sato, K.; Fujitani, S.; Yonezu, I.; Nishio, K. *Acta Mater.* **1997**, *45*, 5213−5221.
(3) Buschow, K. H. J.; Van Der Goot, A. S. *J. Less-Common Met.* **1970**, *22*, 419−428.
(4) Virkar, A. V.; Raman, A. *J. Less-Common Met.* **1969**, *18*, 59−66.
(5) Iwase, K.; Sakaki, K.; Nakamura, Y.; Akiba, E. *Inorg. Chem.* **2013**, *52*, 10105−10111.
(6) Colinet, C.; Pasturel, A. *J. Less-Common Met.* **1987**, *134*, 109−122.
(7) Nakamura, Y.; Nomiyama, T.; Akiba, E. *J. Alloys Compd.* **2006**, *413*, 54−62.
(8) Thompson, P.; Reilly, J. J.; Corliss, L. M.; Hastings, J. M.; Hempelmann, R. *J. Phys. F: Met. Phys.* **1986**, *16*, 675−685.
(9) Lartigue, C.; Le Bail, A.; Percheron-Guegan, A. *J. Less-Common Met.* **1987**, *129*, 65−76.
(10) Ishigaki, T.; Harjo, S.; Yonemura, M.; Kamiyama, T.; Aizawa, K.; Oikawa, K.; Sakuma, T.; Morii, Y.; Arai, M.; Ebata, K.; Takano, Y.; Kasao, T. *Phys. B* **2006**, *385*−*386*, 1022−1024.
(11) Ishigaki, T.; Hoshikawa, A.; Yonemura, M.; Morishima, T.; Kamiyama, T.; Oishi, R.; Aizawa, K.; Sakuma, T.; Tomota, Y.; Arai, M.; Hayashi, M.; Ebata, K.; Komatsuzaki, K.; Asano, H.; Tanaka, Y.; Kasao, T. *Nucl. Instrum. Methods Phys. Res., Sect. A* **2009**, *600*, 189−191.
(12) Harjo, S.; Kamiyama, T.; Torii, S.; Ishigaki, T.; Yonemura, M. *Phys. B* **2006**, *385*−*386*, 1025−1028.
(13) Oishi, R.; Yonemura, M.; Nishimaki, Y.; Torii, S.; Hoshikawa, A.; Ishigaki, T.; Morishima, T.; Mori, K.; Kamiyama, T. *Nucl. Instrum. Methods Phys. Res., Sect. A* **2009**, *600*, 94−96.
(14) Oishi-Tomiyasu, R.; Yonemura, M.; Morishima, T.; Hoshikawa, A.; Torii, S.; Ishigaki, T.; Kamiyama, T. *J. Appl. Crystallogr.* **2012**, *45*, 299−308.
(15) Iwase, K.; Mori, K.; Hishinuma, Y.; Hasegawa, Y.; Iimura, S.; Ishikawa, H.; Kamoshida, T.; Ishigaki, T. *Int. J. Hydrogen Energy* **2011**, *36*, 3062−3066.
(16) Yartys, V. A.; Riabov, A. B.; Denys, R. V.; Sato, M.; Delaplane, R. G. J. *J. Alloys Compd.* **2007**, *408*−*412*, 273−279.
(17) Westlake, D. G. *J. Less-Common Met.* **1983**, *91*, 275−292.
(18) Guzik, M. N.; Hauback, B. C.; Yvon, K. *J. Solid State Chem.* **2012**, *186*, 9−16.
(19) Zhang, Q.; Sun, D.; Zhang, J.; Latroche, M.; Ouyang, L.; Zhu, M. *J. Phys. Chem. C* **2014**, *118*, 4626−4633.
(20) Yartys, V.; Denys, R. *J. Alloys Compd.* **2015**, DOI: 10.1016/j.jallcom.2014.12.091.
(21) Iwase, K.; Terashita, N.; Mori, K.; Tashiro, S.; Yokota, H.; Suzuki, T. *Int. J. Hydrogen Energy* **2014**, *39*, 12773−12777.

DOI: 10.1021/acs.inorgchem.5b01290
Inorg. Chem. 2015, 54, 8650−8655